

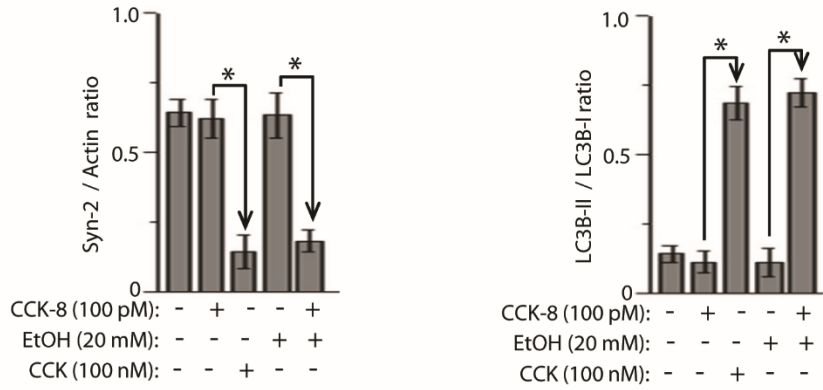
Supplementary Data

Pancreatitis-induced depletion of syntaxin-2 deregulates autophagy and enhances basolateral exocytosis

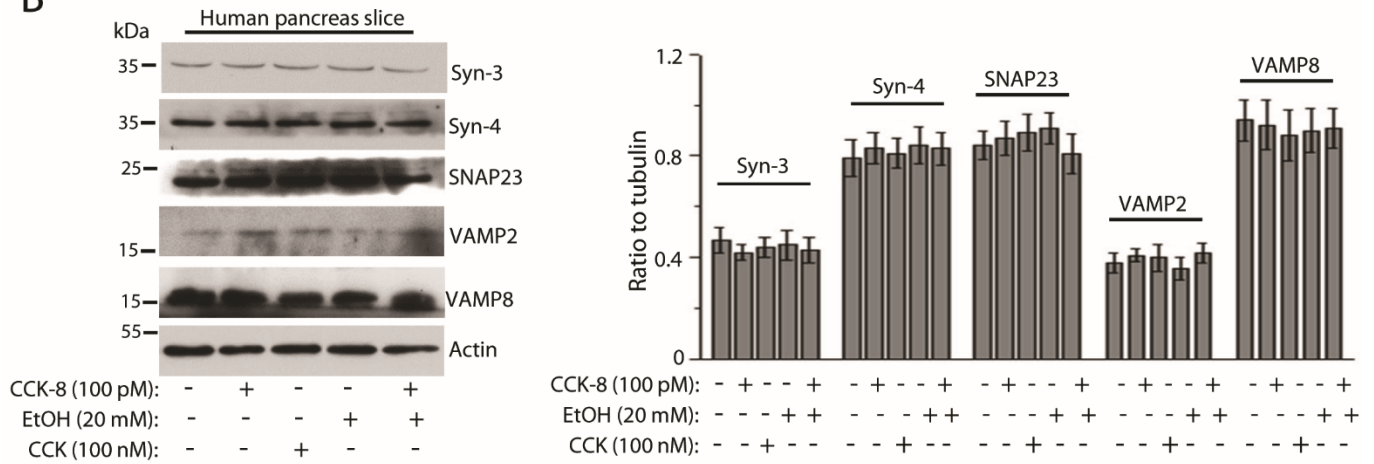
Subhankar Dolai, Tao Liang, Abraham I. Orabi, Douglas Holmyard, Li Xie¹, Dafna Greitzer-Antes, Youhou Kang, Huanli Xie, Tanveer A. Javed, Patrick P. L. Lam, Deborah C. Rubin, Peter Thorn, Herbert Y. Gaisano.

Supplementary Figure 1

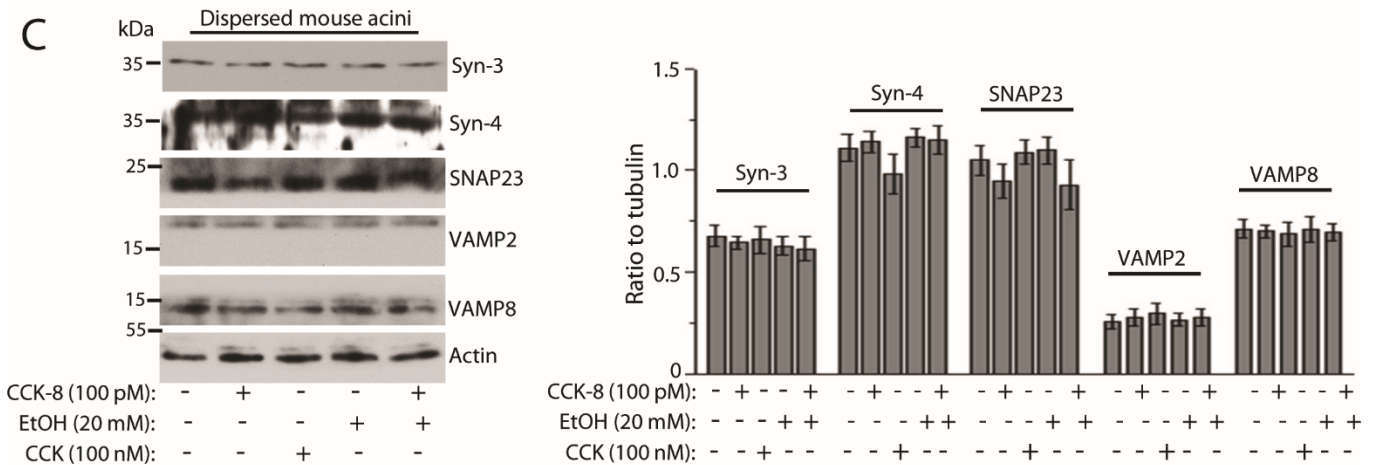
A



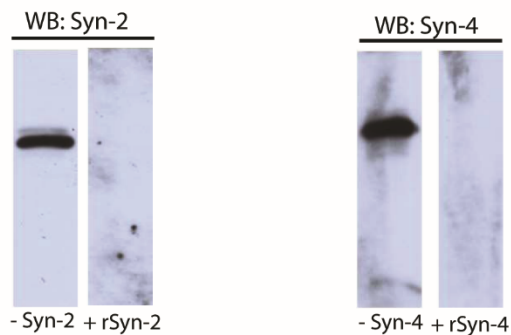
B



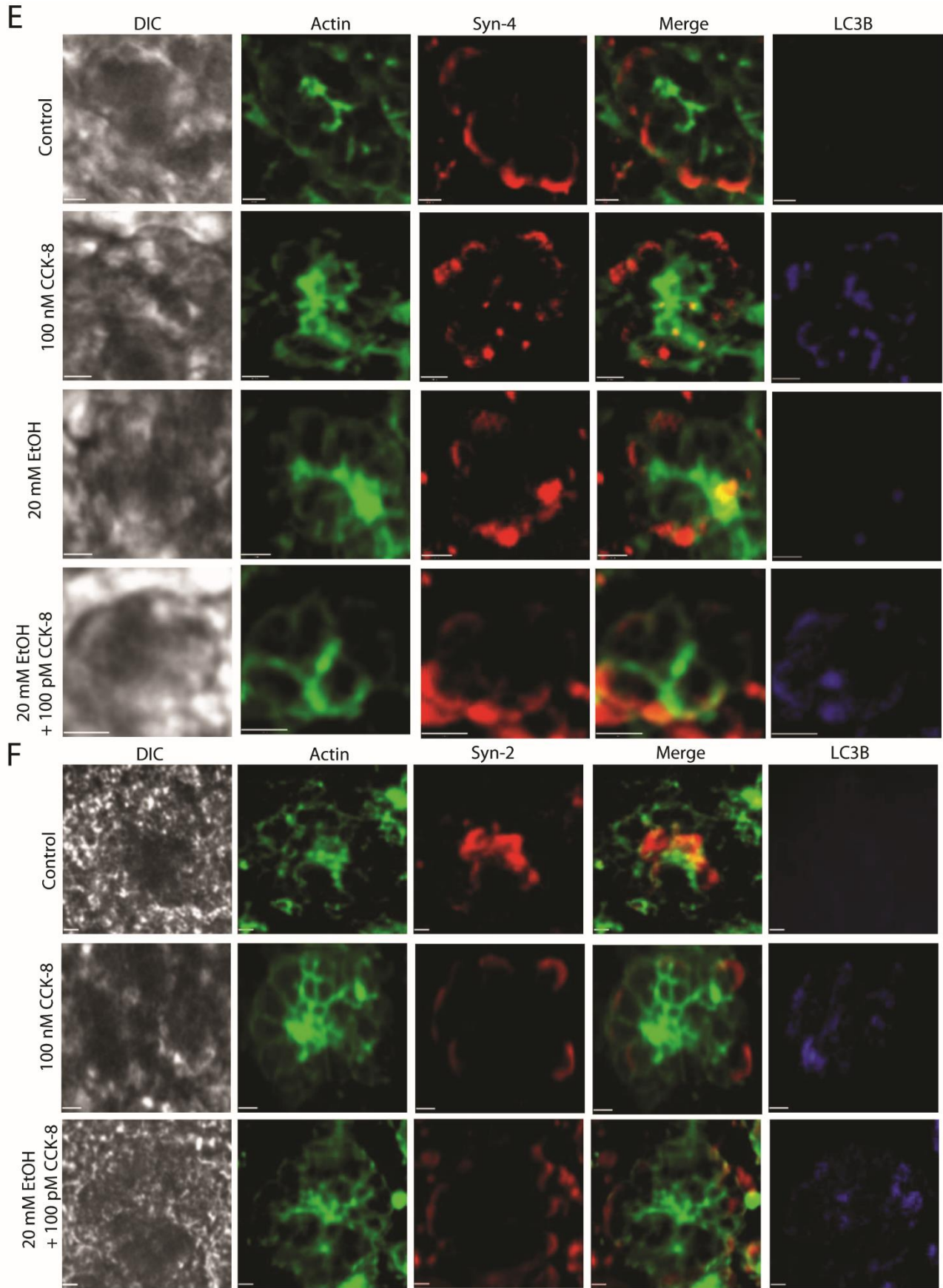
C



D

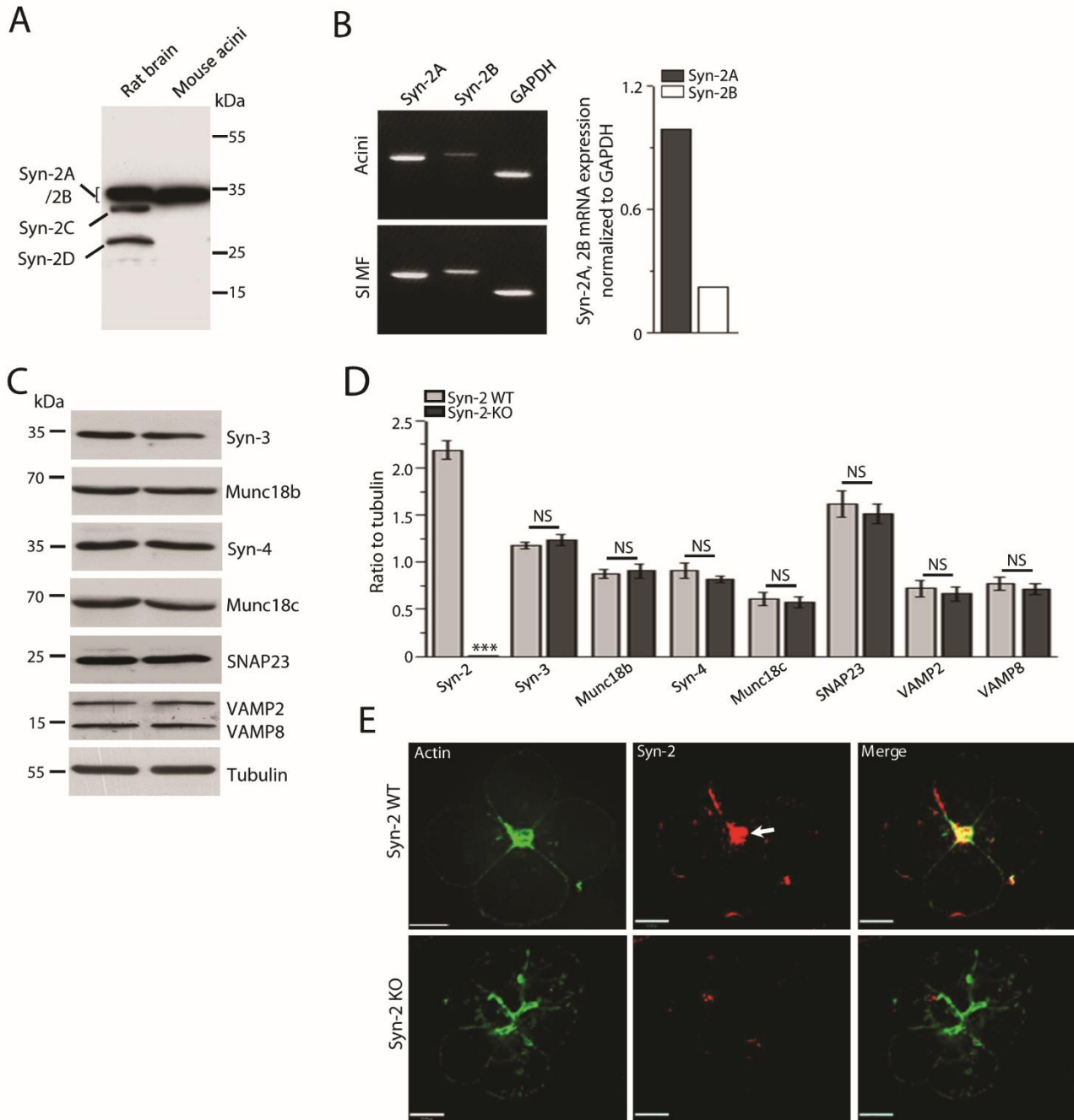


Supplementary Figure 1 Cont.



Supplementary Figure 1. Effects of pancreatitis-inducing treatments on SNARE protein expression in human and mouse exocrine pancreas. (A) *Left*, quantification of Syn-2 (densitometric ratio of Syn-2 to actin) and *right*, LC3B-II transition (densitometric ratio of LC3B-II to LC3B-I) in mouse acini from **Figure 1C**. (B,C) Western blot analysis of lysates of human pancreas slices (in **B**) and mouse acini (in **C**) for SNARE proteins: Syn-3, Syn-4, SNAP23 and VAMPs; actin as loading control. Quantifications of SNAREs (densitometric ratio of SNAREs to actin) are shown in *right* showing no change for the indicated proteins. (D) Verification of the specificity of anti-Syn-2 and Syn-4 antibodies used in all the Western blots of human pancreatic and mouse acinar lysates, and all the confocal imaging studies (examples shown in e and f). Antibodies were used directly (- Syn) or preincubated with excess recombinant Syns (+ rSyn) to probe the blots of human pancreatic lysates. The respective rSyn completely blocked the endogenous Syn (Syn-2 or Syn-4) signal. (E) Pancreatitis-inducing treatments (100 nM CCK-8; 20 mM EtOH + 100 pM CCK-8) have no effects on Syn-4 in human pancreas. Representative immunofluorescence images of human pancreas slices probed for Syn-4, actin (phalloidin) and LC3B (as indicator of autophagic vacuoles) show intact basolateral PM localization of Syn-4 in all indicated conditions, but with appearance of L3C3B-labeled autophagic vacuoles only in the pancreatitis conditions. (F) Another set of representative immunofluorescence images of human pancreas slices probed for Syn-2, actin and LC3B. DIC images are shown to show the intact pancreatic slice tissue. Merge images show abundance (or disruption) of Syn-2 in the apical PM where actin is also most abundant. Data correspond to **Figure 1B**.

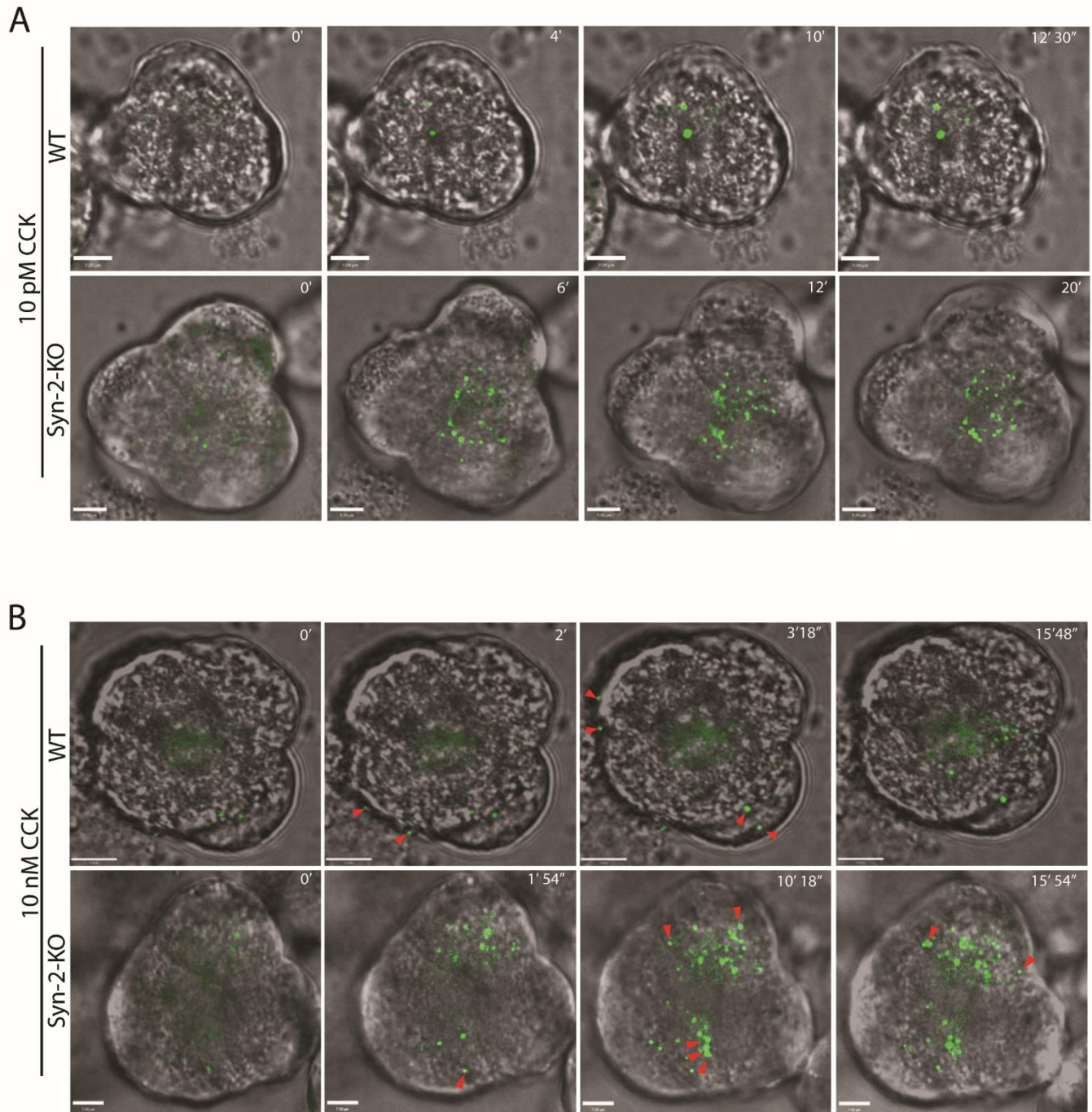
Supplementary Figure 2



Supplementary Figure 2. Syn-2A is the dominant splice variant in mouse pancreatic acini; and Syn-2 deletion does not affect expression of other SNARE and SM proteins. (A) Representative Western blot from 3 independent experiments showing expression of only Syn-2A/-2B splice variants in WT acini. Sprague-Dawley rat brain lysate was used as positive control for all the Syn-2 splice variants (Syn-2A, 2B, 2C and 2D). (B) Representative agarose gels from 2 independent experiments, demonstrating RT-PCR products of Syn-2A/-2B mRNAs from mouse pancreatic acini and mouse small intestinal (SI) myofibroblasts (MF), used as positive control¹ for Syn-2A/-2B splice variants (*left panels*). Relative levels

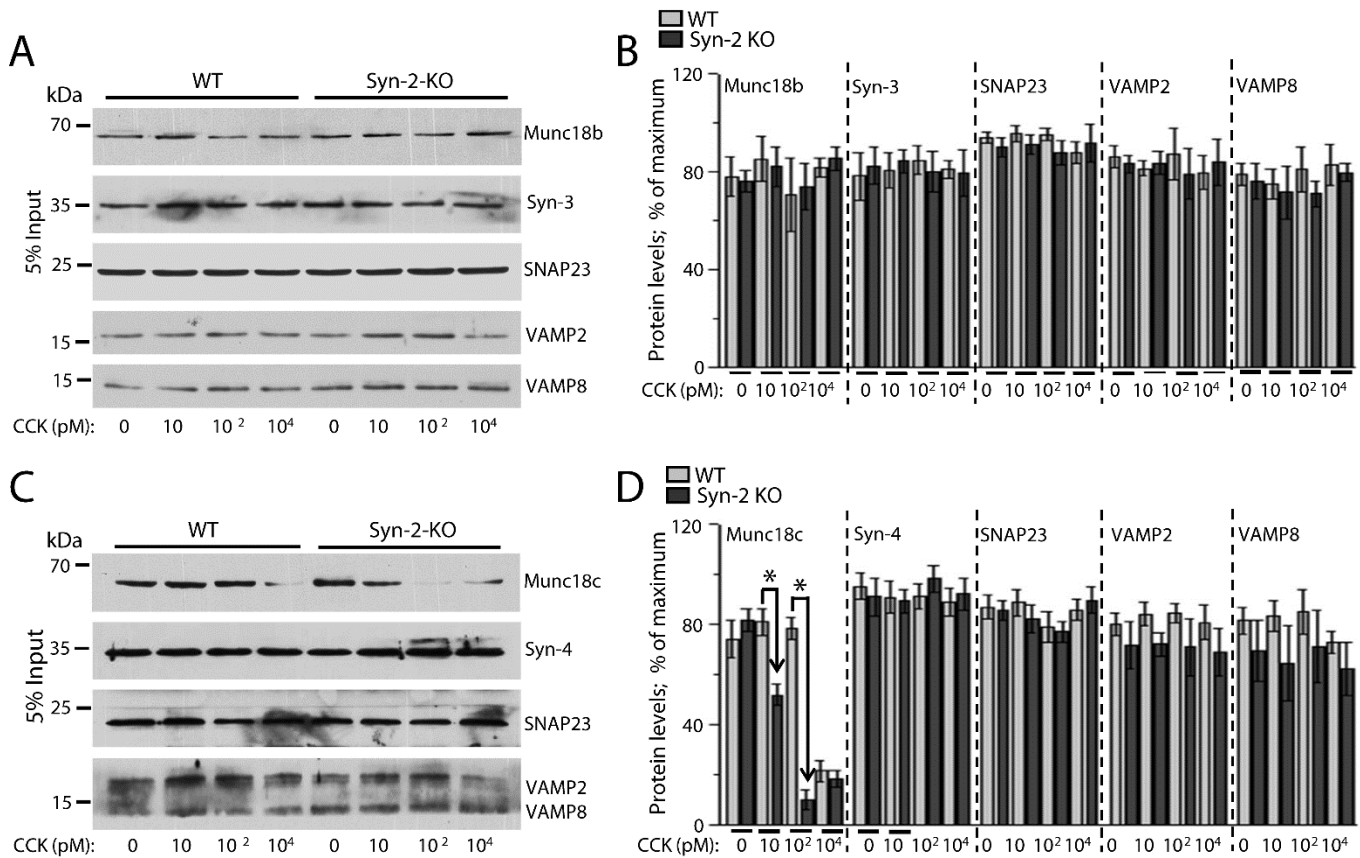
of Syn-2A/-2B mRNA in (B) were quantified by densitometric ratio of RT-PCR products of Syn-2A and Syn-2B to internal loading control GAPDH (*right panel*). (C) Representative Western blots from 3 independent experiments showing expression of indicated proteins in WT and Syn-2-KO acini. Tubulin was used as loading control. (D) Densitometric analysis of band intensities of proteins in (C) and **Figure 2A**. *** $P < 0.001$. (E) Representative confocal images from 3 independent immunofluorescence assays of Syn-2 expression in WT (*top panel*) and Syn-2-KO (*bottom panel*) acini. Acini were double-stained for Syn-2 (*red*) and apical cytoskeleton F-actin (*green*). Arrows in images from *top panel* indicate abundant expression of Syn-2 in apical PM that colocalized (*yellow* in merged image) with apical F-actin. A complete ablation of Syn-2 in Syn-2-KO acini (*bottom panel*) was observed. Scale bar, 10 μm .

Supplementary Figure 3



Supplementary Figure 3. Enlarged images from **Figure 3Ci** (in **A**) and **Figure 3Di** (in **B**) showing the fusion events more clearly. *Red triangles* indicate exocytosis occurring at the basal and lateral plasma membrane. The above four image sequences are shown in real time in movies (10 pM CCK: WT in **Movie-1**, Syn-2 KO in **Movie-2**; 10 nM CCK: WT in **Movie-3**, Syn-2-KO in **Movie-4**).

Supplementary Figure 4

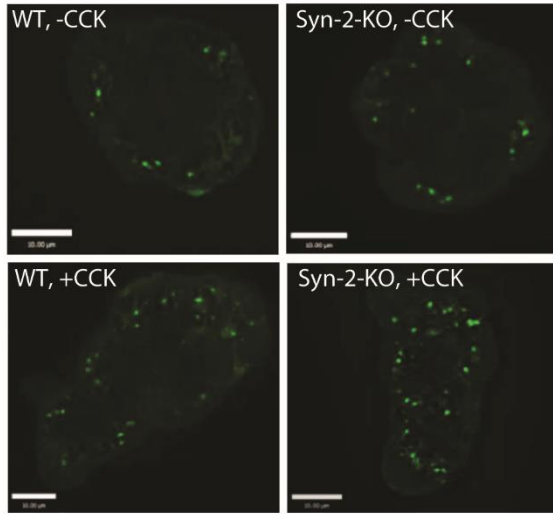


Supplementary Figure 4. Inputs controls corresponding to Figure 4A and B. (A and C) are inputs of Figure 4A and 4B, respectively, shown as representative blots from 3 independent experiments. They show equal expression of the indicated SNARE proteins. Munc18b (in A) and Munc18c (in C) were however affected differently by the different doses of CCK-8. First of all, the activation of the basolateral exocytosis complex involves Munc18c disassembly from its cognate SNARE complex, which we had confirmed^{2,3} in Figure 4B. This was similarly observed with Munc18b disassembly during activation of the apical exocytosis complex in Figure 4A. 50 µg of total acini lysates from corresponding samples were used. Blots were exposed to a similar time as the immunoprecipitation blots in Figure 4A and B. (B and D) Densitometric analyses (Image J, taking maximum band intensity as 100) corresponding to (A) and (C), showing equal SNARE protein levels. Munc18c levels were reduced only after 10nM CCK-8 stimulation in WT acini as previously reported^{2,3}. However, in Syn-2-KO acini, reduced Munc18c levels were also observed after lower doses of 10pm and 100pM CCK-8 stimulation(C and D). In contrast, Munc18b levels were equal and unaltered in all concentrations of CCK-8 (in A and B). These results confirm that Munc18c disassembled from PM-bound Syn-4 and displaced into the cytosol undergoes

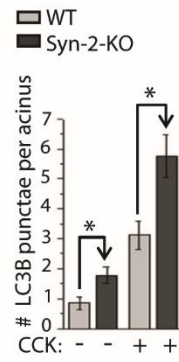
degradation^{2,3}. In contrast, Munc18b disassembled from its cognate Syn-3 and displaced into the cytosol, does not undergo significant degradation. Data are presented as mean \pm s.e.m. *P<0.05.

Supplementary Figure 5

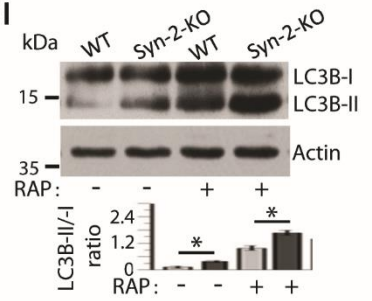
Ai



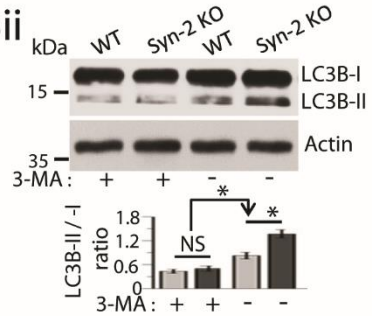
Aii



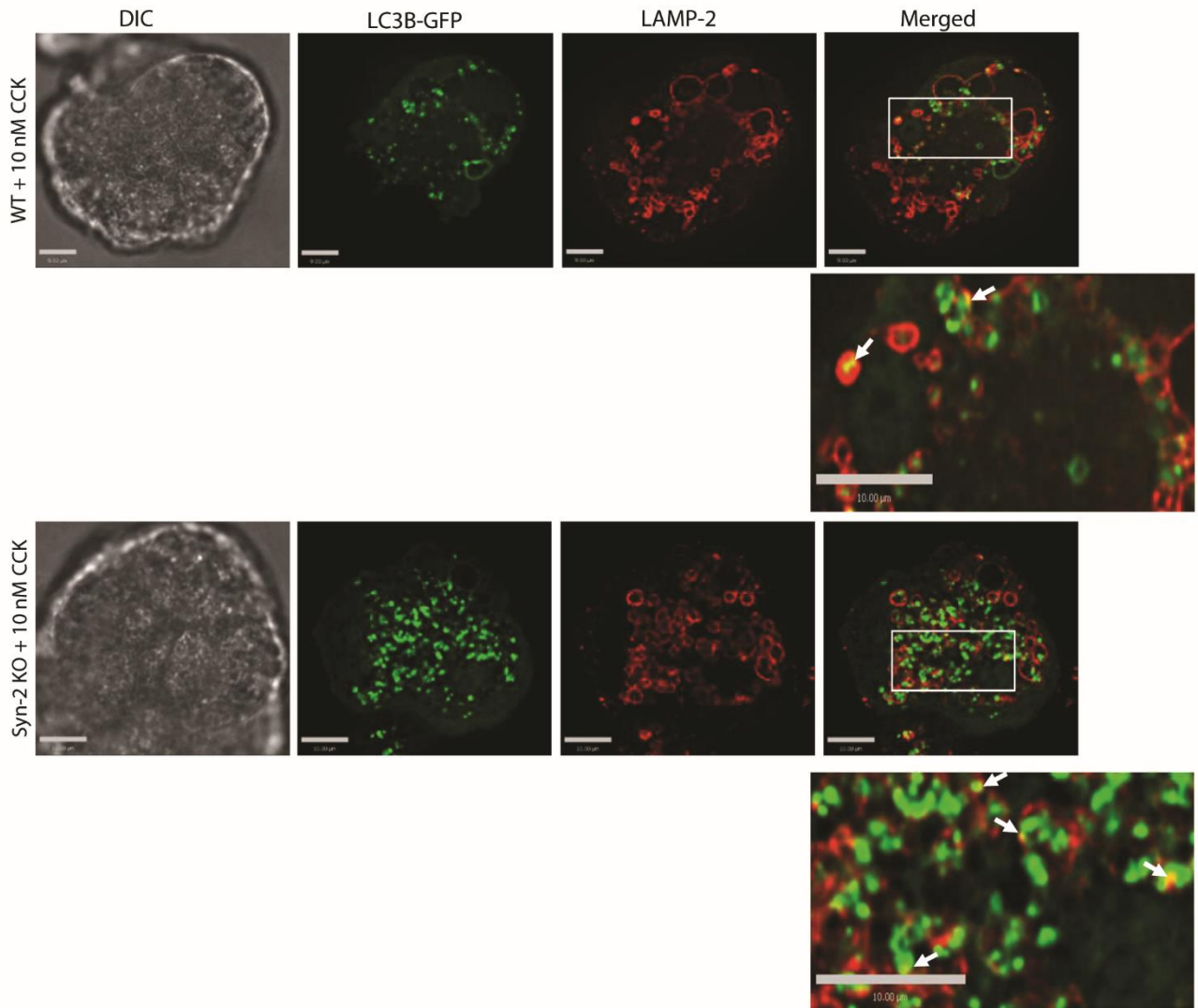
Bi



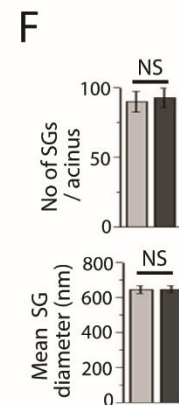
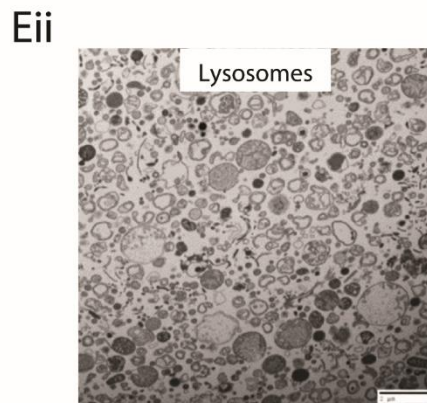
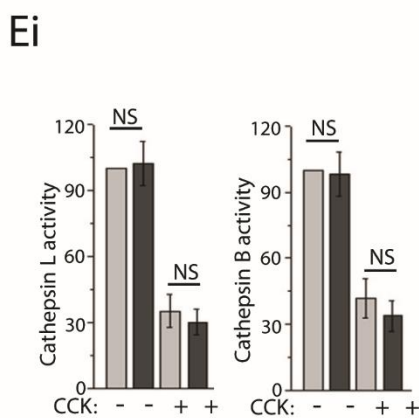
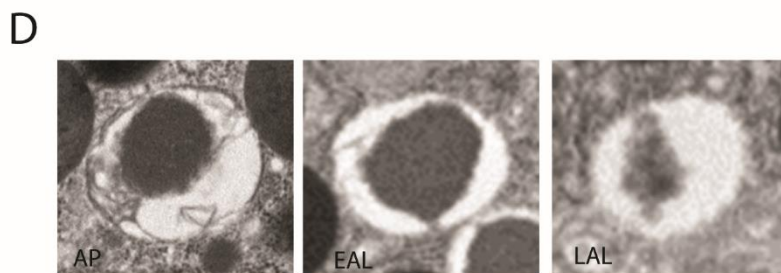
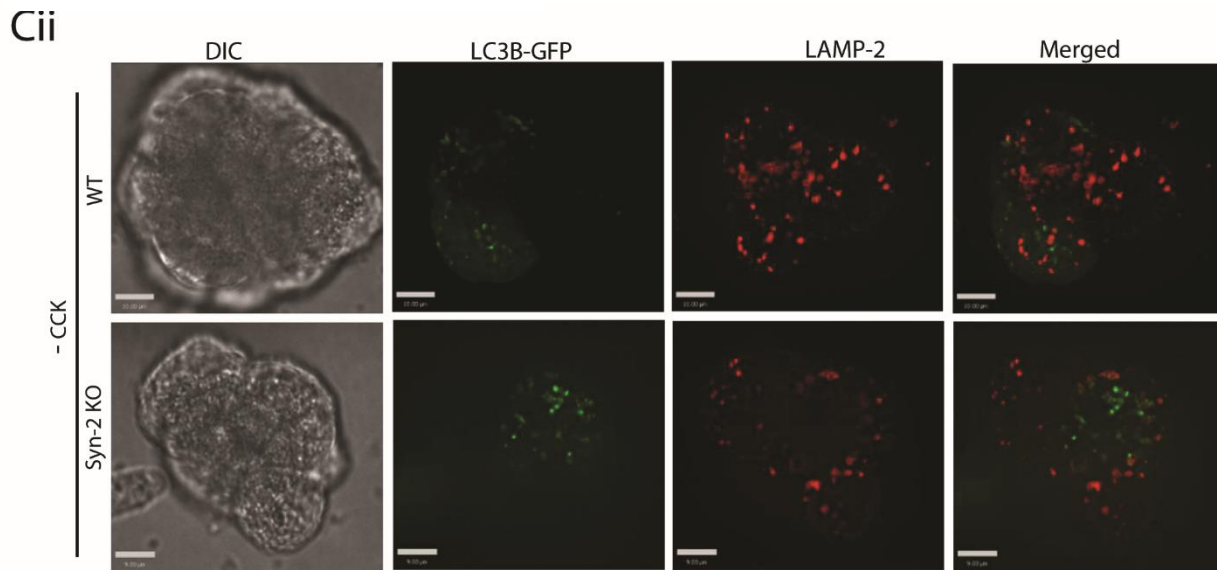
Bii



Ci



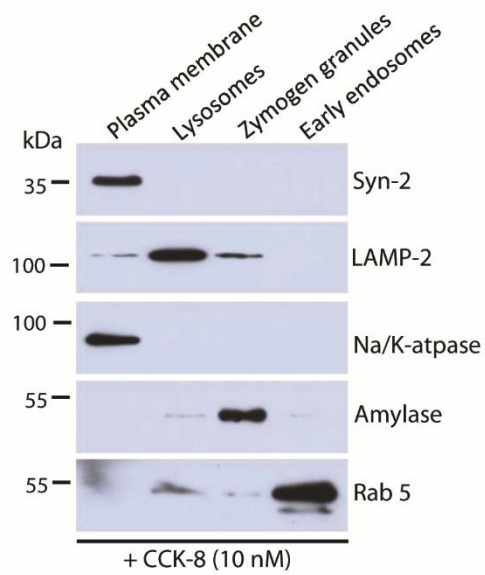
Supplementary Figure 5 Cont.



Supplementary Figure 5. Syn-2 deletion enhances supramaximal CCK-8-induced autophagy which promotes autolysosome accumulation (Ai) Abundance of LC3B-GFP punctae in the pancreatic acini (WT vs Syn-2-KO mice) 12 hr after Ad-LC3B-GFP-transduction in Control condition (no CCK, *top panel*) or stimulated with 10nM CCK-8 (*bottom panel*). **(Aii)** Quantification of LC3B-GFP punctae from 80 acinar cells (at least 20 cells from each experiment) from 3 independent experiments. Data expressed as mean \pm s.e.m. **(Bi)** LC3B-I to LC3B-II transition in Control WT or Syn-2-KO acini cultured for 12 hrs in presence of 150nM rapamycin or **(Bii)** 1mM 3-MA. LC3B-II quantified and expressed as in **Figure 5A bottom**. **(Ci)**

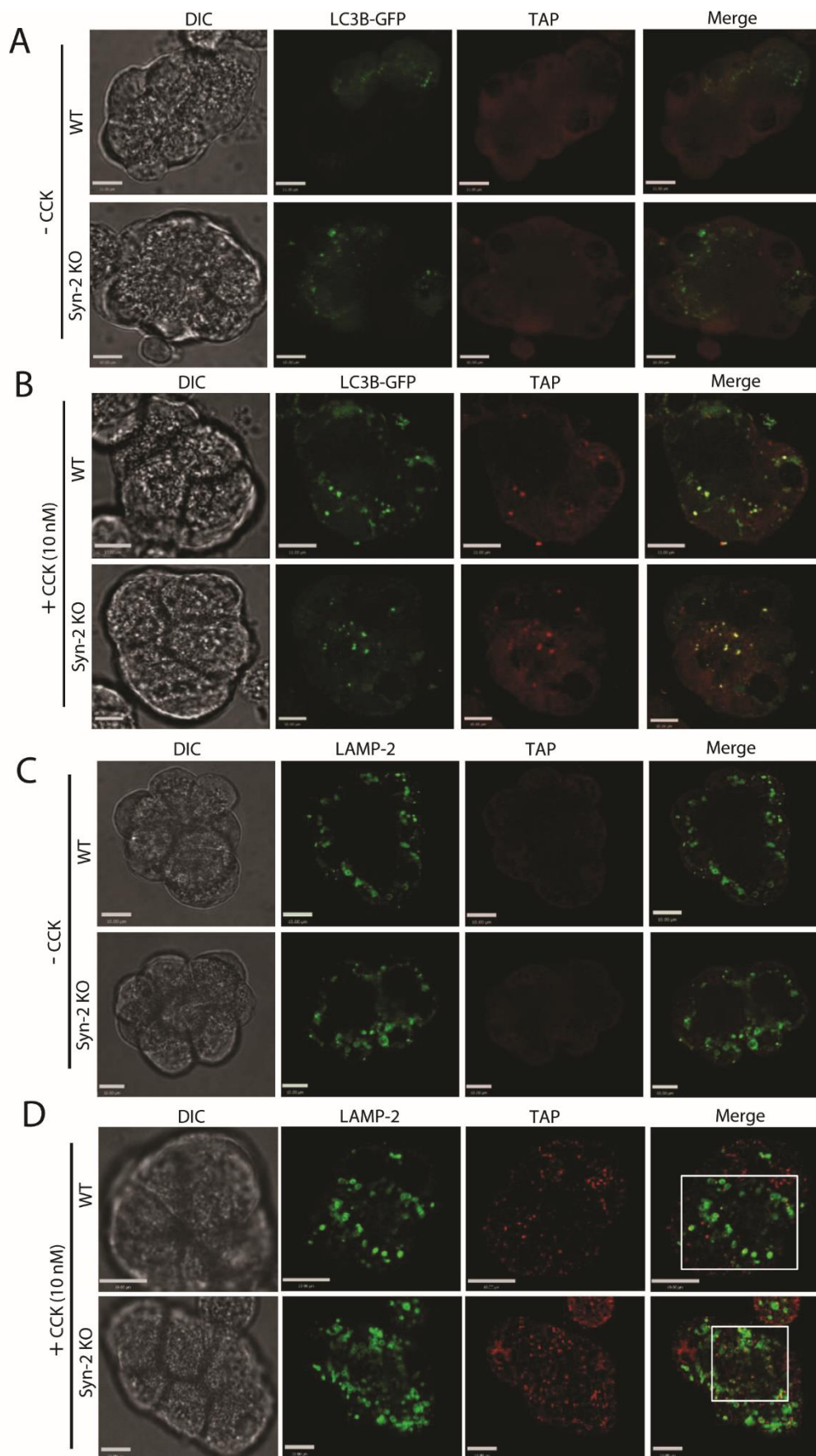
Accumulation of LC3B-GFP in lysosomes was assessed by LAMP-2 immunofluorescence (*red*) in 12 hr post Ad-LC3B-GFP-transduced WT (*top*) and Syn-2-KO acini (*bottom*) followed by 30 min CCK-8 stimulation. **(Cii)** Shown are Control acini. Images are representative from 3 independent experiments. Scale bars, 10 μm . **(D)** Typical examples of distinct acinar AVs, used to quantify in **Figure 5Bii**. **(Ei)** Relative levels of cathepsin L (*left*) and cathepsin B (*right*) activities in the lysosomal fractions. **(Eii)** Purity of lysosomal fraction assessed by EM. **(F)** Quantitation of average number of ZGs and ZG diameter between Syn-2-KO and WT acini. 30 micrographs for each condition from 3 independent experiments were analyzed. Data shown as mean \pm s.e.m.

Supplementary Figure 6.



Supplementary Figure 6. Subcellular fractionation of dispersed WT acini. Acini were stimulated with CCK-8 (10nM) for 30 min followed by fractionation as described in *Methods*. LAMP-2, Na/K⁺-Atpase, Rab5 and amylase were used as markers for lysosomes, plasma membrane, early endosomes and zymogen granules respectively.

Supplementary Figure 7.



Supplementary Figure 7. Complete sequences of confocal images corresponding to **Figure 6Ai** (LC3B-GFP/TAP) in **A** and **B**; and **Figure 6Bi** (LAMP-2/TAP) in **C** and **D**. Only merged images were shown in **Figure 6Ai** and **Figure 6Bi**. Data are representatives from 3 independent experiments. Scale bars: 11 μ m for WT acini and 10 μ m for Syn-2-KO acini.

References:

1. Wang Y, Wang L, Iordanov H, et al. Epimorphin(-/-) mice have increased intestinal growth, decreased susceptibility to dextran sodium sulfate colitis, and impaired spermatogenesis. *J Clin Invest* 2006;116:1535-46.
2. Dolai S, Liang T, Lam PP, et al. Effects of ethanol metabolites on exocytosis of pancreatic acinar cells in rats. *Gastroenterology* 2012;143:832-43 e1-7.
3. Gaisano HY, Lutz MP, Leser J, et al. Supramaximal cholecystokinin displaces Munc18c from the pancreatic acinar basal surface, redirecting apical exocytosis to the basal membrane. *J Clin Invest* 2001;108:1597-611.

Supplementary Materials and Methods

Pancreatitis-induced depletion of syntaxin-2 deregulates autophagy and enhances basolateral exocytosis

Subhankar Dolai, Tao Liang, Abraham I. Orabi, Douglas Holmyard, Li Xie¹, Dafna Greitzer-Antes, Youhou Kang, Huanli Xie, Tanveer A. Javed, Patrick P. L. Lam, Deborah C. Rubin, Peter Thorn, Herbert Y. Gaisano.

Mouse Genetics.

WT (syntaxin-2^{+/+}) and Syn-2-KO (syntaxin-2^{-/-}, homozygous mutant) mice were obtained from crossing of syntaxin-2^{+/+} and kept at 22°C, 40% humidity, 12:12-h light–dark cycle and given chow and water *ad libitum*. Mice were genotyped as reported¹. In all experiments, experimental mice were compared with age and sex-matched littermate controls of the same genetic background (C57BL6).

Reagents.

Fura-2 AM, Pluronic F-127, Alexa Fluor 488-phalloidin and FM1-43 were from Molecular Probes (Eugene, OR). Substrate for trypsin (Boc-Gln-Ala-Arg-MCA) and chymotrypsin (Suc-Ala-Ala-Pro-Phe-AMC) were from Peptides International (Louisville, KY) and Calbiochem (San Diego, CA), respectively. Syncollin-pHluorin adenovirus was generated by us². CCK-8 was from Research Plus (Barnegat, NJ). Sulfated caerulein, a decapeptide analogue of the pancreatic secretagogue CCK-8 and all other reagents unless specified were from Sigma (St Louis, MO).

Reverse transcription-PCR.

For semi-quantitative reverse transcription PCR (RT-PCR), total RNA was extracted using TRIzol reagent (Invitrogen, Burlington, ON); after which, a 1.5 µg sample was reverse transcribed using OneStep RT-PCR kit (Qiagen, Hilden, Germany). PCR amplification was carried out for 30 cycles with the following primers to detect Syntaxin-2A/-2B: Syntaxin-2A/-2B forward, 5'-ATGCGGGACCGGCTGCCCCGAC-3'; Syntaxin-2A reverse, 5'-TGCCAACCGACAAGCCAATGATTAG-3'; and Syntaxin-2B reverse, 5'-TGACAATGCTGTTGCGAGAATAATTC-3'. Integrity of the cDNAs was confirmed by amplifying glyceraldehyde-3-phosphate dehydrogenase (GAPDH) using following primers: GAPDH forward, 5'-AACATCATCCCTGCATCCAC-3' and GAPDH reverse, 5'-GACAACCTGGTCCTCAGTGT-3'. 8 µL of amplified

products were then subjected to 2.0% agarose gel electrophoresis and stained with ethidium bromide to visualize on UV-transilluminator.

Acinar Isolation and Culture, Adenovirus Transduction, HEK293 Cell Culture and Transfection.

Dispersed pancreatic lobules (15-20 cells) and small acini (3-6 cells) were prepared using excised pancreata from adult (2-4 months) mice by a mechanical and enzymatic dissociation technique as described earlier² using Krebs-Ringer-HEPES (KRH) buffer (NaCl 104, KCl 5, KH₂PO₄ 1, MgCl₂ 1.2 and HEPES 25; in mM, pH 7.4) supplemented with 1.2 mM CaCl₂, 2.5 mM D-glucose, 2 mM L-glutamine, MEM amino acids (Invitrogen, Burlington, ON, Canada), MEM nonessential amino acids (Invitrogen), 0.015% (wt/vol) soybean trypsin inhibitor, and 0.2% (wt/vol) BSA. Cells were dissociated by a process of mechanical dissociation in a shaking water bath (37°C, 100 rpm) and enzymatic digestion (130–240 units of CLSPA-grade collagenase; Worthington, Lakewood, NJ), followed by trituration and filtering through a 212- μ m filter. Acini were plated on poly-L-lysine coated coverslips and cultured overnight in DMEM/F12 media supplemented with 10% normal goat serum, 100 units/ml penicillin, and 100 μ g/ml streptomycin at 37°C in a humidified incubator containing 5% CO₂. For viral transduction 10¹⁰ pfu/ml adenovirus was added to the culture 12 hr prior to imaging or other experiments.

Human embryonic kidney 293 (HEK293) cells were cultured (at 37°C within 5% CO₂) in Dulbecco's modified Eagle medium (DMEM) supplemented with 10% fetal bovine serum, 100 units/ml penicillin and streptomycin, 2 mM L-glutamine were seeded at a density of 1 \times 10⁶ cells per 60-mm dish. Transient transfections were performed the following day with pcDNA3.1-Syn-2/ -Syn-3/ -Syn-4 or pcDNA3.1-Syn-2 in combination with pcDNA3.1-Syn-3/ -Syn-4/ pLJM1-FLAG-Atg16L1 isoform 1 or pBrain-GFP-CHC(1-1675) (1.5 μ g plasmid DNA per construct per 60 mm plate) using Lipofectamine 2000 (Thermo-Fisher, Watham, MA), as described in the manufacturer's protocol and processed for GST pull-down and immunoprecipitation analysis 48 hr post-transfection.

Human Pancreas Slice Preparation

Portions of human pancreas were obtained from the Surgical Pathology Laboratory of the Toronto General Hospital. Healthy portions of the pancreas were retrieved from resected pancreas of patients (5 patients; 3 males and 2 females, ages ranging from 60 to 70 years old) with pancreatic cancer, whose written consent was obtained. Pancreas tissue slices (80- μ m thick) were prepared in ice-cold

extracellular solution (ECS in mM: 125 NaCl, 2.5 KCl, 1 MgCl₂, 2 CaCl₂, 1.25 NaH₂PO₄, 26 NaHCO₃, 2 sodium pyruvate, 0.25 ascorbic acid, 3 *myo*-inositol, 6 lactic acid, 7 glucose) with a vibrating blade microtome (VT-1000S, Vibratome; Leica Microsystems, Mannheim, Germany) as described recently³.

Enzyme Assays.

Amylase secretion from dispersed mice pancreatic acini were assayed using a colorimetric method⁴. ~10⁶ isolated acini were resuspended in KRH buffer and stimulated with minimal to supramaximal concentrations of CCK-8 in 37°C with constant shaking for 1 hr at 37°C. Amylase content of the supernatant and acini pellet was determined and results of amylase secretion are expressed as percentage of total amylase, which is the sum of amylase content in the supernatant and acini pellet. Serum amylase, lipase and pancreatic myeloperoxidase (MPO) activities were determined with commercially available kits (Biovision, Milpitas, CA) as per manufacturer's instructions using 5 µl of serum and 100 µg of volume adjusted (4 µg/µl) pancreatic tissue lysates. Trypsin and chymotrypsin activity was measured in pancreatic acini/tissue homogenates by a fluorimetric assay we've described⁵. Briefly, agonist stimulated acini or pancreatic tissues were either sonicated or homogenised in 1:5 (w/v) trypsin assay buffer (in mM: 50 Tris, pH 8.1, 150 NaCl, 1 CaCl₂; 0.01% BSA) on ice and subjected to centrifugation at 1000 g for 1 min. 50 µl of each postnuclear supernatant were added to wells of a 96-well black µ-clear plates (Greiner Bio-One, Kremsmunster, Austria) containing 50 µl of trypsin assay buffer and mixed well. 50 µl of 400 µM enzyme substrate were then added to sample containing wells. Release of protease cleaved 7-amino-4-methylcoumarin (AMC) was measured immediately at room temperature over 10 minutes using a fluorescent plate reader (Fluostar Optima, Isogen Life Science, De Meern, Netherlands). Protease activity was collected as relative fluorescent units/second, normalized to total amylase (relative fluorescent units/second/microgram of amylase), and expressed as a fold increase relative to either the control or a maximum condition. Lysosomal cathepsin L (CL) and cathepsin B (CB) activities were assessed by CL/CB Activity Assay kits (#ab65306/#ab65300, Abcam) according the manufacturer's protocol with some modifications. Briefly, lysosomal pellets were solubilized in 1:5 (W/V) ice-cold CL/CB buffers and 10 µL of lysates from each condition were added to 90 µL of CL/CB buffer in in 96-well black µ-clear plates. Lysates were incubated with 200 µM of CL substrate Ac-FR-AFC or CB Substrate Ac-RR-AFC for 2 hrs in presence or absence of CL/CB inhibitor (in 1:50 dilution). CL/CB activity was measured by the release of AFC (amino-4-trifluoromethyl coumarin)

using a fluorimeter (as described above) at 400 nm excitation, and 460 nm and 505 nm emission for CL and CB respectively. The relative fluorescent units (RFU) were normalized with protein concentrations, and RFU of lysosomal CL/CB was determined by subtracting the RFU measured in the presence of CL/CB inhibitor. Data expressed as percentage of change in activity taking WT control lysosomal activity as 100.

Intracellular Calcium ($[Ca^{2+}]_i$) Measurement.

This was performed similar to our previous report⁶. Pancreatic lobules were loaded with ratiometric Ca^{2+} indicator Fura-2 AM (1.0 μ M with 0.05% pluronic F-127) for 30 min at room temperature in an extracellular solution (ECS, in mM): NaCl 135, KCl 5, $MgCl_2$ 1, $CaCl_2$ 1, glucose 10, NaOH-HEPES 10, pH 7.4, followed by washing with ECS and incubation for a further 30 min for dye deesterification. Lobules were plated on poly-L-lysine coated coverslips and imaged on a Zeiss inverted epifluorescence microscope (Oberkochen, Germany). Acini were sequentially illuminated through 340/25 nm and 380/25 nm excitation filters and imaged through 40X UV, 1.3 NA, oil immersion objective through a 500/20 nm longpass filter. 512 pixel x 512 pixel images were captured at 3 frames/s with 35 ms exposure on a *Hamamatsu Flash 4.0* cooled CCD camera (Hamamatsu Photonics, Hamamatsu City, Shizuoka, Japan). A 340/380 ratio (R) that is proportional of $[Ca^{2+}]_i$ was calculated for each image after background subtraction for each wavelength. Calibration of intracellular Fura-2 signal was performed using ECS with no Ca^{2+} (+1 mM EGTA) to obtain minimum ratio (R_{min}) and with high Ca^{2+} (+10 mM $CaCl_2$) to obtain maximum ratio (R_{max}) of 340/380 in presence of ionomycin (1 μ M). The intracellular R of Fura-2 was then converted to $[Ca^{2+}]_i$ using the formula $[Ca^{2+}]_i = K_d * [(R - R_{min}) / (R_{max} - R)] * S_f / S_b$, where S_f and S_b is the emission intensity at 380 nm for Ca^{2+} -free and Ca^{2+} -bound Fura-2, respectively. The system was driven and images were quantified by Volocity 3DM software (Perkin Elmer, Waltham, MA). Data and statistical analysis were performed in EXCEL (Microsoft, Redmond, WA).

Immunoprecipitation (IP), GST pull-down and Western blot analysis.

IP was performed similarly we've reported⁴. Briefly, treatments were stopped immediately by adding 2 volumes of ice-cold KRH buffer. Acini were then washed 2X with ice-cold PBS, harvested by centrifugation (300g, 4°C) and lysed by sonication in lysis buffer (25 mM HEPES, 100 mM KCl, 1.5% Triton X 100 with protease inhibitors). 1 mg of protein extract from each condition were initially precleared with 50 μ L of protein A/G-sepharose beads (Molecular Probes, Eugene, OR) for 2 hr at 4°C

and then subjected to IP with specific 2 µg anti-Syn-2 (#110022), Syn-3 (#110033), Syn-4 (#110042) from SySy (Goettingen, Germany); 4 µg anti-Atg16L1 (#8089S, Cell Signaling Technology, Danvers, MA) or anti-FLAG (F3165, M2; Sigma) antibodies linked to protein A/G-sepharose beads.

GST pull-down was performed as reported earlier⁷. GST and GST-linked full-length VAMP2 and VAMP8 were purified using glutathione-Sepharose beads from BL21 (DE3) Escherichia coli, transformed with appropriate constructs in pGEX plasmids. 48-h post-transfected HEK293 cells, transformed with Syn-2 alone or in combination with Syn-3/-4 were washed with PBS and lysed in binding buffer (20 mM HEPES, 100 mM KCl, 1.5% Triton X-100, 1 mg/ml leupeptin, 10 mg/ml aprotinin; pH 7.4) at 4°C. Lysates were clarified (21,000g, 30 min, 4°C) and 400 mg of soluble supernatant mixed with 200 pmol of glutathione-agarose beads bound to GST-VAMP2, GST-VAMP8, or GST (as negative control), at 4°C with constant agitation for 2 hr.

Beads obtained from IP or GST pull-down were washed three times with ice-cold lysis buffer and eluted from the beads by boiling in sample buffer (2 M Tris/HCl, pH 6.8, 20% SDS, 30% glycerol, 0.03% phenol red). Eluted proteins from Syn-3 and Syn-4 IPs were separated on 12-15% gradient SDS-PAGE while 10% SDS-PAGE was used for Syn-2, Atg16L1 and FLAG IPs and 13% SDS-PAGE was used for GST pull-down samples, followed by electrophoretic transfer onto nitrocellulose membrane (Millipore Corp., Bedford, MA). Membranes were immune-decorated with appropriate primary antibodies and identified by standard Western blot analysis technique with an ECL enhanced chemiluminescence detection kit (GE Healthcare, Burlington, ON, Canada). Primary antibodies used were anti-Syns (1:1,000), anti-SNAP23 (111202, SySy; 1:1,000), anti-Munc18b (1:1,000)⁴, anti-Munc18c (AF5659, R&D Systems, Minneapolis, MN); 1:200), anti-VAMP2 (1:200) (19,22), anti VAMP8 (1:500) (19,22), anti-Beclin-1 (#4122S, 1:1000), anti-LC3B (#2775S, 1:800) from Cell Signaling Technology; anti-Clathrin (#610499, BD Bioscience, San Jose, CA); 1:1,000), anti-Atg16L1 (M150-3, MBL; 1.5 µg/mL), anti-FLAG (4 µg/mL), anti-GFP (632375, Living Colors (Takara Bio, Mountain View, CA; 1:1500); anti-LAMP2 (ab13524, Abcam); anti-Rab5a (NBP1-20255, Novus Biologicals, Littleton, CO) anti-Amylase (1:2000), anti-Actin (1:5,000) and anti-Tubulin (1:5,000) from Sigma.

Spinning Disc Confocal Microscopy.

All imaging experiments in this study described below were performed with a spinning disc confocal imaging system composed of an Olympus IX81 inverted fluorescence microscope (Center Valley, PA), a

Yokogawa CSU X1 spinning disc confocal scan head (Yokogawa Electric Corporation, Tokyo, Japan), a diode-pumped solid state laser set (405 nm, 491 nm, 561 nm, 605 nm) (Spectral Applied Research, Concord, ON, Canada), and a Hamamatsu C9100-13 EM-CCD (Hamamatsu Photonics, Shizuoka, Japan). Images were captured at a magnification of 94.3X (63X oil immersion objective, 1.35 NA). This system was driven and image data analyzed by Volocity 3DM software (Perkin Elmer Corporation, Waltham, MA). All images were deconvolved using specific point spread function (confidence limit=95%, iteration limit=20) and noise was removed.

Immunofluorescence Microscopy.

Freshly prepared or LC3-B-GFP transduced and agonist stimulated acini, and human pancreas slices were fixed in 4% paraformaldehyde in PBS for 1 hr, and permeabilized in 0.1% Triton X-100 buffer for 20-60 min. Samples were then blocked 1 hr in 10% goat serum and immunostained with the primary antibody to Syn-2 (#ab12369), LAMP2 (#ab13524), Abcam (Cambridge, UK; 1:100), Syn-4 (1:100), LC3B (sc-16755, Santa Cruz Biotechnology, Santa Cruz, CA, 1:200) or anti-TAP antibody (ABIN1173333, Antibodies Online, Atlanta, GA); 1:100). Samples were washed with PBS to remove unbound antibodies, and incubated with Alexa Fluor 594-conjugated anti-rabbit or Alexa 647-conjugated anti-goat (Jackson ImmunoResearch (West Grove, PA), 1:500)/ Alexa Fluor 488-conjugated anti-rat (Abcam) secondary antibody. F-actin was detected with Alexa Fluor 488-conjugated Phalloidin. Samples were further washed with PBS and then mounted with fluorescent mounting medium (DakoCytomation, Glostrup, Denmark). 0.4 μm thick optical sections were captured with 0.3 μm Z-spacing.

FM1-43 Imaging.

Exocytosis imaging using the FM1-43 dye (Thermo-Fisher) was performed as we had previously reported^{4, 8}. Dispersed acini, plated on glass coverslips were mounted in a thermal chamber (37°C, 5% CO₂), and treated with 5 μM FM1-43 for ~15 min until a stable basal fluorescence level was attained. Time lapsed imaging (15 min) was performed with the above system and images acquired at 6 frames/min with 50 msec exposure time. Region of interests (ROIs) encompassing entire apical or constant width encompassing the basal plasma membrane were drawn and intensity changes of FM1-43 fluorescence within ROIs were normalized to the intensity at basal state and expressed as mean intensity changes /2 μm^2 PM with time.

Syncollin-pHluorin Imaging.

This was performed as we've previously described^{2,4} on cultured acini that transduced with Syncollin-pHluorin adenovirus. All stimulations were done using sulfated CCK-8 in KRH buffer in a heated chamber equilibrated at 37°C. Images were acquired with 491 nm laser at 6 frames/min for 15 min.

Electron Microscopy.

This was performed essentially as we've described earlier^{4,9}. Briefly, agonist stimulation was terminated by adding 2 volumes of ice-cold KRH buffer. The acini were then pelleted and washed 2X by centrifugation (300 g, 4 °C) with ice-cold PBS, fixed immediately with a Karnovsky style fixative (3.2% paraformaldehyde and 2.5% glutaraldehyde, in a buffer containing, in mM: 0.1 sodium cacodylate, 5 CaCl₂, pH 6.5) for 1 hr and then postfixed with 1% osmium tetroxide for 30 min. Samples were pre-embedded in 1% uranyl acetate for 1 hr, were then dehydrated and infiltrated with Epon 812 resin. Completion of polymerization of the epoxy resin resulted in a solid epoxy disk, which was subjected to ultrathin sectioning (80 nm) using a Reichert Ultracut microtome, and collected on 200 mesh copper grids. The sections were counterstained for 15 min each, using saturated 4% uranyl acetate followed by Reynold's lead citrate and then examined and photographed in a Hitachi H-7000 transmission electron microscope (Tokyo, Japan) at an accelerating voltage of 75 kV, by using an AMT XR-60 camera and AMT software. ZGs diameter were measured (ImageJ; <http://rsb.info.nih.gov/ij>) on scale-adjusted micrographs.

Subcellular fractionation. Acini were fractionated to enriched ZGs and lysosomes by differential centrifugation^{10,11}, and to enriched PM using sucrose density gradient¹² with slight modifications using a SW40Ti rotor (Beckman) at 4°C. Briefly, acini were prepared from three pancreases for each condition (Control or CCK-8 stimulation). Control and agonist stimulated acini were pelleted at 500 rpm at 4°C. Pellets were resuspended in 0.3M sucrose solution (1:10 acini to sucrose, w/v), and homogenised three times using a glass homogenizer. The lysates were equally divided into two tubes and one was subjected to organelle fractionation, where unbroken cells and nuclei were pelleted at 200g, 15 min. Resultant supernatant were spun at 1300g, 15 min to obtain ZG fraction. Post-ZG supernatants were pelleted at 12,000g, 12 min to obtain lysosome and mitochondria enriched fraction; post 12,000g supernatants were considered as endosomal fraction. PM fractions were obtained from second portion of the lysates

that was centrifuged at 1000g for 12 mins. Resultant pellet was resuspended to 1:10 (w/v) 0.3M sucrose solution. Sucrose density were adjusted to 1.58M with 2M sucrose solution, layered with 0.3M sucrose and subjected to sucrose gradient centrifugation at 25000 rpm for 60 min¹² to obtain PM fraction at the 1.58M/0.3M interface. Each fraction was solubilized in to 1:10 (w/v) lysis buffer and 20 µg of each were used for Western blot analysis.

Induction of Experimental Pancreatitis, Preparation of Serum and Tissue Samples and Scoring of Caerulein-Induced Acinar Injury.

These assays were performed similar to our previous report⁹. For caerulein-induced acute pancreatitis, age (2-4 months) matched male littermate mice weighing 20-25 g were fasted for 18 hrs with free access to water. Caerulein was solubilized in 0.9% saline at a concentration of 2.5 µg/ml and administered as eight intraperitoneal (i.p.) injections at a dose of 50 µg/kg body weight at hourly intervals. Mice from control groups received equal volume of 0.9% saline. Mice were sacrificed 1 hr after the 8th injection of caerulein. Whole blood samples were collected by puncturing the heart with heparin coated syringe and centrifuged at 4°C. Plasma was stored at -80°C for further studies. The pancreata were removed on ice and divided in to three parts. One part was fixed in 10% formalin solution in PBS and paraffin embedded for histological assessment. Remaining two parts were frozen immediately in liquid nitrogen and stored in -80°C for biochemical assays.

To evaluate necrosis after caerulein-induced pancreatitis in the pancreas of WT control and Syn-2-deficient mice, formalin-fixed samples were embedded in paraffin and 5 µm sections (3 sections, each 50 µm apart) were stained with hematoxylin and eosin (H&E). Slides were scanned with a slide scanner (Axioscan, Zeiss, Oberkochen, Germany) at 40X magnification and images scored by an experienced morphologist. The intensity of necrosis was scored as the product of lesion severity (on a 0–3 scale) to their extension (in percentage of surface involved (1 = 0–25%; 2 = 25–50%; 3 = 50–75%; 4 = 75–100%) leading to a 0–12 scale. In a similar way, intensity of inflammation was scored as the product of the degree of neutrophil infiltration (on a 0–3 scale) to the extension of infiltration evaluated as above.

Densitometric Analyses.

ImageJ 1.49t software from <http://rsbweb.nih.gov/ij/download> was used to quantify intensities of the bands obtained in Western blots and RT-PCR.

Statistics.

Statistical analyses were performed by one-way analysis of variance (ANOVA) using ORIGIN (Microcal, Amherst, MA) or 2-tailed Student's t-test using EXCEL (Microsoft). Data presented as means \pm s.e.m. $P < 0.05$ considered statistically significant.

Study Approval.

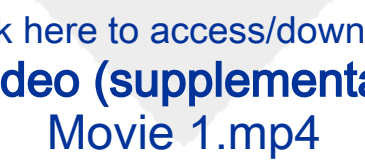
Animal procedures were performed in accordance with the University of Toronto's Animal Care Committee's ethical guidelines. All procedures involving human pancreas tissues were approved by the Research Ethics Boards of the University Health Network of Toronto and University of Toronto.

References

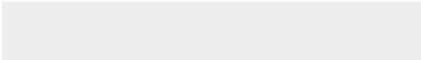

1. Wang Y, Wang L, Jordanov H, et al. Epimorphin(-/-) mice have increased intestinal growth, decreased susceptibility to dextran sodium sulfate colitis, and impaired spermatogenesis. *J Clin Invest* 2006;116:1535-46.
2. Fernandez NA, Liang T, Gaisano HY. Live pancreatic acinar imaging of exocytosis using syncollin-pHluorin. *Am J Physiol Cell Physiol* 2011;300:C1513-23.
3. Liang T, Dolai S, Xie L, et al. Ex vivo human pancreatic slice preparations offer a valuable model for studying pancreatic exocrine biology. *J Biol Chem* 2017;292:5957-5969.
4. Dolai S, Liang T, Lam PP, et al. Effects of ethanol metabolites on exocytosis of pancreatic acinar cells in rats. *Gastroenterology* 2012;143:832-43 e1-7.
5. Orabi AI, Shah AU, Muili K, et al. Ethanol enhances carbachol-induced protease activation and accelerates Ca²⁺ waves in isolated rat pancreatic acini. *J Biol Chem* 2011;286:14090-7.
6. Thorn P, Lawrie AM, Smith PM, et al. Local and global cytosolic Ca²⁺ oscillations in exocrine cells evoked by agonists and inositol trisphosphate. *Cell* 1993;74:661-8.
7. Dolai S, Xie L, Zhu D, et al. Synaptotagmin-7 Functions to Replenish Insulin Granules for Exocytosis in Human Islet beta-Cells. *Diabetes* 2016;65:1962-76.
8. Gaisano HY, Lutz MP, Leser J, et al. Supramaximal cholecystokinin displaces Munc18c from the pancreatic acinar basal surface, redirecting apical exocytosis to the basal membrane. *J Clin Invest* 2001;108:1597-611.
9. Cosen-Binker LI, Binker MG, Wang CC, et al. VAMP8 is the v-SNARE that mediates basolateral exocytosis in a mouse model of alcoholic pancreatitis. *J Clin Invest* 2008;118:2535-51.

10. Saluja A, Saito I, Saluja M, et al. In vivo rat pancreatic acinar cell function during supramaximal stimulation with caerulein. *Am J Physiol* 1985;249:G702-10.
11. Tartakoff AM, Jamieson JD. Subcellular fractionation of the pancreas. *Methods Enzymol* 1974;31:41-59.
12. Meldolesi J, Jamieson JD, Palade GE. Composition of cellular membranes in the pancreas of the guinea pig. I. Isolation of membrane fractions. *J Cell Biol* 1971;49:109-29.

Title: Real time imaging of apical exocytosis in WT acini
stimulated with physiologic 10 pM CCK-8.



Click here to access/download
Video (supplemental)
Movie 1.mp4

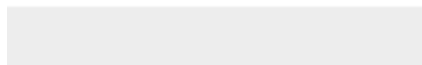




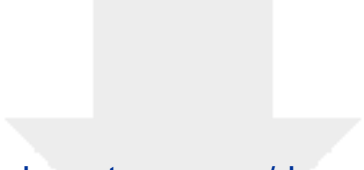
[Click here to access/download](#)

Video (supplemental)

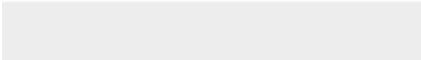

Movie 2.mp4



Title: Real time imaging of basolateral exocytosis in WT acini
stimulated with supraphysiologic 10 nM CCK-8.



Click here to access/download
Video (supplemental)
Movie 3.mp4



Title: Real time imaging of exaggerated basolateral and unblocked apical exocytosis in Syn-2-KO acini stimulated with 10 nM CCK-8.

